TU Delft

Delft University of Technology

Document Version
Final published version

Licence
CC BY

Citation (APA)
Chang, B. L., & Van Mieghem, P. (2026). Classical mean-field epidemic theory upper-bounds real disease spread. *Communications Physics*, *9*(1), Article 320. https://doi.org/10.1038/s42005-026-02723-3

Important note
To cite this publication, please use the final published version (if applicable).
Please check the document version above.

Copyright
In case the licence states “Dutch Copyright Act (Article 25fa)”, this publication was made available Green Open Access via the TU Delft Institutional Repository pursuant to Dutch Copyright Act (Article 25fa, the Taverne amendment). This provision does not affect copyright ownership.
Unless copyright is transferred by contract or statute, it remains with the copyright holder.

Sharing and reuse
Other than for strictly personal use, it is not permitted to download, forward or distribute the text or part of it, without the consent of the author(s) and/or copyright holder(s), unless the work is under an open content license such as Creative Commons.

Takedown policy
Please contact us and provide details if you believe this document breaches copyrights.
We will remove access to the work immediately and investigate your claim.

*This work is downloaded from Delft University of Technology.*

communications physics

A Nature Portfolio journal

Article

https://doi.org/10.1038/s42005-026-02723-3

# Classical mean-field epidemic theory upper-bounds real disease spread

Check for updates

Brian L. Chang ✉ & Piet Van Mieghem

Non-Markovian theory provides the most accurate stochastic description of an infection spreading on a contact graph with a general distribution of the infection time and curing time. However, the infection time is not directly measurable and instead the generation time is measured in real-world epidemics. Here we show that if the generation time follows approximately a Weibull distribution with shape parameter $\alpha$, then the Weibull infection time of the spreading process possesses a similar shape parameter $\alpha$. For a large list of published generation times in biological, mainly respiratory epidemics, the Weibull shape parameter $\alpha$ is computed, which reveals that nearly always $\alpha > 1$. The impact of this observation is that a complicated non-Markovian analysis is not needed, because the well-established Markovian case $\alpha = 1$ provides a lower bound for the epidemic threshold and an upper bound for the basic reproduction number and the nodal infection probabilities in the contact graph.

In most countries, academic groups together with public health agencies have been advising their governments during the the recent COVID-19 pandemic. In hindsight, the COVID-19 crisis has been remarkably well-managed in general, given that the computational methods were essentially based on the surprisingly simple SIR epidemic model. The main control parameter for the agencies was the basic reproduction number $R_0$: if $R_0 < 1$, then the epidemic is "under control", else actions are needed. While more accurate physical descriptions of epidemic spread in a time-variant contact graphs exist, our key message here is that the development of a difficult non-Markovian theory for epidemics on networks can be avoided for biological respiratory diseases. However, the comfortable and reassuring fact that a complicated non-Markovian theory is not needed, does not generally hold for non-biological spread in e.g. social contagion and information diffusion via online platforms.

The class of Susceptible-Infected-Susceptible (SIS) epidemics is the simplest compartmental model of a disease spread with re-infections in a population, in which individuals are either infectious (I) or healthy, but susceptible (S). The class of Susceptible-Infected-Removed (SIR) epidemics is the companion compartment model without re-infections, which adds the removed (R) compartment next to the I and S compartment. The SIR model [1, p. 713-716] arose first as a constant rate simplification of the more general Kermack-McKendrick theory of epidemics. Other compartmental models[2] can be described, both stochastically and deterministically (after a mean-field approximation), similarly to SIS/SIR epidemics. The SIR class is upper bounded in the nodal infection probability and in the basic reproduction number by its SIS companion[3,4], which justifies our confinement to SIS theory and the omission of an SIR analysis here. From a physical and mathematical point of view, the Markovian SIS process on a graph is the simplest and still analytically tractable model in the class of "Local rule, Global emergence" (LrGe), that contains many physical processes such as Lotka-Volterra predator-prey, Kuramoto synchronization, opinion dynamics and others in e.g. [5, Sec. 1]. Most LrGe processes feature a phase transition.

The viral spreading process in SIS epidemics is described by the infection time $T_{\text{inf}}$ while in real-world epidemics, the generation time $T_{\text{gen}}$ is measured. We assume that the infection time $T_{\text{inf}}$ and generation time $T_{\text{gen}}$ can both be described by Weibull distributions. The Weibull distribution has a shape parameter $\alpha > 0$ and reduces to an exponential distribution for $\alpha = 1$. A large literature survey of published generation time measurements in biological epidemics reveals that the generation time shape parameter $\alpha_{\text{gen}} > 1$ in most cases. We show that a generation time shape parameter $\alpha_{\text{gen}} > 1$ implies an infection time shape parameter $\alpha_{\text{inf}} > 1$. Since the nodal infection probability decreases with $\alpha$ and the epidemic threshold which is inversely proportional[6] to the basic reproduction number $R_0$ increases with $\alpha$, we conclude that Markovian epidemics $\alpha = 1$ upper-bound the infection probability in real-world biological diseases, which supports our main message: current epidemic models, computed by most agencies, provide a safe-side overestimation of the real disease impact.

## Methods

### Markovian SIS epidemics on a graph

The contact graph $G$ consists of a set of $N$ individuals, called nodes in the graph, and $L$ contacts as links in the graph. For simplicity, we assume here that the graph is fixed and does not change over time (a Markov theory of time-varying contact graphs exists, see e.g.[7,8]). The graph $G$ is described by the adjacency matrix $A$, where the element $a_{ij} = 1$ if there is a link between node $i$ and node $j$, and $a_{ij} = 0$ otherwise.

Delft University of Technology, Faculty of Electrical Engineering, Mathematics and Computer Science, Delft, The Netherlands. ✉e-mail: B.L.Chang@tudelft.nl

At any time $t$ in the SIS epidemic, each node is in one of two states: susceptible or infectious. There are two independent stochastic processes in the SIS model: the infection process is described by the infection time $T_{\text{inf}}$, and the curing process is described by the curing time $T_{\text{cure}}$.

The infection process determines the time at which an infectious node $i$ spreads the disease to a susceptible node $j$, which can only occur if there is a link between node $i$ and node $j$. In Markovian epidemics, an infectious node $i$ infects a susceptible neighbor $j$ at a constant rate $\beta$, which implies that the infection time $T_{\text{inf}}$ is an exponentially distributed random variable with mean $\mathbb{E}\left[T_{\text{inf}}\right] = \frac{1}{\beta}$. Similarly, the curing process determines the time at which an infectious node $i$ recovers from the disease. In Markovian epidemics, an infectious node $i$ recovers from the disease at a constant rate $\delta$, which implies that the curing time $T_{\text{cure}}$ is an exponentially distributed random variable with mean $\mathbb{E}\left[T_{\text{cure}}\right] = \frac{1}{\delta}$.

Markovian SIS epidemics are fully parameterized by the infection rate $\beta$, the curing rate $\delta$, and the contact graph $G$ and can be described exactly by a Markov chain with $2^N$ states [9, Ch. 17.2.1]. The viral state of a node $i$ at time $t$ in a Markovian SIS process on a graph is specified by a Bernoulli random variable $X_i(t) \in \{0, 1\}$: the viral state $X_i(t) = 0$ for a susceptible node and $X_i(t) = 1$ for an infected node. The fact that the Markov state $X_i(t)$ in SIS epidemics is a Bernoulli random variable facilitates an elegant and physical differential equation for the infection probability of node $i$, first proposed in[10],

$$\frac{\mathrm{d}\mathbb{E}[X_i]}{\mathrm{d}t} = \mathbb{E}\left[-\delta X_i + \beta(1 - X_i)\sum_{k=1}^{N} a_{ki}X_k\right] \tag{1}$$

$$= -\delta\mathbb{E}[X_i] + \beta\sum_{k=1}^{N} a_{ki}\mathbb{E}[X_k] - \beta\sum_{k=1}^{N} a_{ki}\mathbb{E}[X_iX_k] \tag{2}$$

The time-derivative of the infection probability $\mathbb{E}\left[X_i\right] = \Pr\left[X_i = 1\right]$ of a node $i$ consists of the expectation of two competing processes in (1), expressed in the Bernoulli random variable $X_i \in \{0, 1\}$: (i) if node $i$ is infected $X_i = 1$, then the node $i$ is cured at rate $\delta$, else (ii) if node $i$ is susceptible $X_i = 0$, then all infected neighbors $\sum_{k=1}^{N} a_{ki}X_k$ of node $i$ try to infect the node $i$ with rate $\beta$. The last term in (2), containing joint probabilities $\mathbb{E}\left[X_iX_k\right] = \Pr\left[X_i = 1, X_k = 1\right]$, is complicating and requires us to deduce the differential equation for $\mathbb{E}\left[X_iX_j\right]$, which is found in [9, Ch. 17.3]. The resulting differential equation for $\frac{\mathrm{d}\mathbb{E}\left[X_iX_j\right]}{\mathrm{d}t}$ contains the joint probabilities $\mathbb{E}\left[X_iX_jX_k\right]$ of the triples. Continuing in this manner as shown in [9, Ch. 17.3], we arrive at the $2^N$ linear differential equations.

Many interesting insights from (1) can be deduced. First, a powerful mean-field approximation, called $N$-Intertwined Mean Field Approximation (NIMFA)[11], explained in[12], follows from (1) by replacing the random variable $X_i$ by its simplest approximation, its mean $v_i(t) = \mathbb{E}\left[X_i\right]$,

$$\frac{\mathrm{d}v_i(t)}{\mathrm{d}t} = -\delta v_i(t) + \beta(1 - v_i(t))\sum_{j=1}^{N} a_{ij}v_j(t) \tag{3}$$

Since the NIMFA differential equation (3) is an approximation, $\mathbb{E}\left[X_i\right]$ is written instead of $\mathbb{E}\left[X_i\right]$. The accuracy of NIMFA in (3) is assessed in[13]. Second, the NIMFA epidemic threshold $\tau_c^{(1)} = \frac{1}{\lambda_1}$ in [11, Lemma 6], where $\lambda_1$ is the largest eigenvalue or spectral radius[14] of the adjacency matrix $A$, is proved in[15] to be a lower bound for the Markovian epidemic threshold, i.e. $\tau_c > \tau_c^{(1)}$. Also[3], the NIMFA infection probability $v_i(t) = \Pr\left[X_i(t) = 1\right]$ upper-bounds the Markovian probability of infection $\Pr\left[X_i(t) = 1\right]$. Further, NIMFA has been extended to a large variety of compartmental models in[2], exact solutions of the NIMFA differential equation (3) on the complete graph are derived in[16] and analytic solutions around the epidemic threshold in terms of a hyperbolic tangent function are deduced in[17].

## Non-Markovian SIS epidemics on a graph

In non-Markovian SIS epidemics, the infection time $T_{\text{inf}}$ and curing time $T_{\text{cure}}$ can take any distribution. We limit ourselves here to a Weibull distribution with probability density function (pdf) [9, p. 56]

$$f_{\text{Weibull}}(x) = \frac{\alpha}{b}\left(\frac{x}{b}\right)^{\alpha-1} \mathrm{e}^{-\left(\frac{x}{b}\right)^{\alpha}} \tag{4}$$

with shape parameter $\alpha$ and scale parameter $b$. The Weibull distribution is a good fit for many empirical distributions[18] and appears often in epidemic papers (e.g.[19–22]).

In general, the parameter $\alpha$ is the extreme value index [9, p. 398] of a probability distribution. Small changes in $\alpha$ lead to highly different behavior. If the parameter $\alpha \neq 1$, small $x$-values in the corresponding pdf tend to either 0 (for $\alpha > 1$) or infinity (for $\alpha < 1$). Only if $\alpha = 1$, the distribution is regular and possesses a Taylor series around $x = 0$. In particular, if $\alpha = 1$, then the Weibull distribution reduces to an exponential distribution, recovering the Markovian case. The parameter $\alpha$ also determines the fractional order of linear differential equations[23, Ch. 1], whose eigenfunctions are Mittag-Leffler functions $E_{\alpha,b}(z) = \sum_{k=0}^{\infty}\frac{z^k}{\Gamma(\alpha k+b)}$, which are entire functions in the complex $z$-plane of order $\frac{1}{\alpha}$ and $E_{1,1}(z) = \mathrm{e}^z$. Again, slightly different values of $\alpha$ lead to widely different asymptotic behavior of entire functions. The resulting $\alpha$-process in continuous time, described as a linear combination of Mittag-Leffler functions with different $b$, features $\alpha$-power law behavior for small and large times. The Mittag-Leffler distribution $1 - E_{\alpha,1}(-x^{\alpha})$ behaves similarly[23, art. 101] as the Weibull distribution $1 - e^{-x^{\alpha}}$ for not too large $x > 0$ and the same $0 < \alpha \leq 1$. For $\alpha = 1$, the Mittag-Leffler distribution again reduces to the exponential distribution. In summary, the parameter $\alpha$ is a characteristic measure for non-Markovian behavior of a process.

For a random variable $T$, the hazard function $h_T(x) = \frac{f_T(x)}{S_T(x)}$ where $f_T(x)$ is the probability density function and $S_T(x) = \Pr[T > x] = 1 - F_T(x)$ is the survival function. The hazard function of a Weibull random variable is given by

$$h_{\text{Weibull}}(x) = \frac{\alpha}{b}\left(\frac{x}{b}\right)^{\alpha-1} \tag{5}$$

The hazard function $h(x)$ represents the instantaneous event rate at time $x$ given that the event has not yet occurred by time $x$. Hence, the instantaneous rate at which an infectious node $i$ recovers from the disease at time $x$ is given by the hazard function $h_{T_{\text{cure}}}(x)$ of the curing time $T_{\text{cure}}$. Similarly, the instantaneous rate at which an infectious node $i$ spreads the disease to a susceptible neighbor $j$ is given by the hazard function $h_{T_{\text{inf}}}(x)$ of the infection time $T_{\text{inf}}$ (under the so-called "rule 2" infection process defined by Boguñá et al.[24]). For shape parameter $\alpha = 1$, the Weibull distribution reduces to the exponential distribution and the hazard function (5) becomes constant, recovering the Markovian case.

Weibull infection time $T_{\text{inf}}$ dramatically alters the SIS epidemic dynamics. The viral spreading process is very sensitive to the infection time shape parameter $\alpha_{\text{inf}}$. Decreasing the infection time shape parameter $\alpha_{\text{inf}}$ leads to a significant increase in the prevalence as reported in[15] and[24]. The Weibull hazard function $h_{T_{\text{inf}}}(x)$ at small times $x$ increases when the shape parameter $\alpha_{\text{inf}}$ decreases, which allows the virus to spread faster and leads to a higher prevalence. The epidemic threshold also decreases as shown in[15]. Therefore, the shape parameter $\alpha_{\text{inf}}$ characterizes the non-Markovian behavior. If $\alpha_{\text{inf}} \neq 1$, the process is non-Markovian, with smaller shape parameters corresponding to faster-spreading epidemics with higher prevalence. If the infection time shape parameter $\alpha_{\text{inf}} > 1$, then the Markovian case $\alpha_{\text{inf}} = 1$ provides a lower bound for epidemic threshold $\tau_c$, which is in turn lower bounded by the NIMFA epidemic threshold $\tau_c^{(1)} = \frac{1}{\lambda_1}$. NIMFA therefore provide a safe-side overestimate of the epidemic process.

## Results

### Generation time in SIS epidemics

Direct measurement of the infection time $T_{\text{inf}}$ is not possible, both in real epidemics as well as SIS epidemics. When an infectious node $i$ is in contact with a susceptible node $j$, the infection time $T_{\text{inf}}$ determines when node $i$ will infect node $j$. However, the infection may possibly not occur, because either (i) another node $k$ infects node $j$ or (ii) node $i$ cures before node $i$ can infect node $j$. In reality, we can only observe infections that have actually occurred. Instead, the generation time $T_{\text{gen}}$ is measured, defined as the time between the infection of the primary and secondary case[25]. As illustrated in Fig. 1, node $i$ becomes infected and is the primary case. Node $i$ then infects node $j$, the secondary case. The time between the infection events is the generation time.

Since the time of infection is typically not known, the generation time is approximated by the serial interval, defined as the time between the onset of symptoms in the primary and secondary case. While generation times are always positive, serial intervals may be negative if people transmit the disease before symptom onset (Fig. 1). While the mean serial interval is a good estimator for the mean generation interval, the variance and other central moments differ[25], and these differences impact model predictions[26].

We deduce the distribution of generation time $T_{\text{gen}}$ in SIS epidemics on networks and its relation to the infection time $T_{\text{inf}}$ and curing time $T_{\text{cure}}$. The probability density function $f_{T_{\text{gen}}}(x)$ of the generation time $T_{\text{gen}}$ is related to the basic reproduction number $R_0$ by

$$f_{T_{\text{gen}}}(x) = \frac{m(x)}{R_0} \tag{6}$$

where $m(x)$ is the so-called "infectivity profile", defined as the average rate at which an infected individual infects new individuals at time $x$ after his/her infection[27,28]. Let $M(x) = \int_0^x m(x)\,\mathrm{d}x$ denote the expected number of secondary infections caused by an infectious node $i$ up to time $x$ after node $i$ becomes infected at time 0. Let $\Lambda(x)$ denote the expected number of secondary infections caused by an infectious node $i$ up to time $x$ after node $i$ becomes infected, conditioned on the fact that node $i$ has not cured by time $x$. If the curing time $T_{\text{cure}} > x$, which occurs with survival probability $S_{T_{\text{cure}}}(x) = 1 - F_{T_{\text{cure}}}(x) = \Pr[T_{\text{cure}} > x]$, the expected number of secondary infections before time $x$ is $\Lambda(x)$. If the curing time $T_{\text{cure}} = v < x$, then the expected number number of secondary infections before time $x$ is $\Lambda(v)$. Hence,

$$M(x) = S_{T_{\text{cure}}}(x)\Lambda(x) + \int_0^x f_{T_{\text{cure}}}(v)\Lambda(v)\,\mathrm{d}v \tag{7}$$

The total expected number of secondary infections caused by an infectious node is thus the basic reproduction number $R_0 = \lim_{x\to\infty} M(x)$, which we assume is finite. The distribution function $F_{T_{\text{gen}}}(x) = \Pr[T_{\text{gen}} < x]$ of the generation time is the fraction of secondary infections which occur before time $x$,

$$F_{T_{\text{gen}}}(x) = \frac{M(x)}{R_0} \tag{8}$$

The probability density function $f_{T_{\text{gen}}}(x)$ follows as the derivative

$$f_{T_{\text{gen}}}(x) = \frac{\mathrm{d}}{\mathrm{d}x} F_{T_{\text{gen}}}(x) = \frac{\lambda(x) S_{T_{\text{cure}}}(x)}{R_0} \tag{9}$$

where $\lambda(x) = \frac{\mathrm{d}}{\mathrm{d}x}\Lambda(x)$ is the instantaneous rate at which an infectious node $i$ produces infections at time $x$, given that node $i$ has not cured yet. The infectivity profile in the SIS model is thus $m(x) = \lambda(x) S_{T_{\text{cure}}}(x)$.

In order to obtain the probability density function $f_{T_{\text{gen}}}(x)$, it is sufficient to find any function $\widehat{\lambda}(x)$ which is proportional to $\lambda(x)$, because the same pdf is obtained after normalizing the area to 1. As discussed in the previous section, the hazard function $h_{T_{\text{inf}}}(x) = \frac{f_{T_{\text{inf}}}(x)}{S_{T_{\text{inf}}}(x)}$ represents the instantaneous rate at which an infectious node $i$ infects a susceptible neighbor $j$ at $x$ time units after node $i$ was infected (given that node $i$ has not cured). Therefore, assuming that the number of susceptible neighbors is constant in time, the instantaneous rate at which an infectious node $i$ produces secondary infections is proportional to the hazard function: $\widehat{\lambda}(x) = h_{T_{\text{inf}}}(x)$. Under this assumption, the density function $f_{T_{\text{gen}}}(x)$ of the generation time in a Weibull SIS process follows as

$$f_{T_{\text{gen}}}(x) = \frac{1}{\Gamma\left(\frac{\alpha_{\text{inf}}}{\alpha_{\text{cure}}}\right)} \frac{\alpha_{\text{cure}}}{b_{\text{cure}}} \left(\frac{x}{b_{\text{cure}}}\right)^{\alpha_{\text{inf}}-1} \mathrm{e}^{-\left(\frac{x}{b_{\text{cure}}}\right)^{\alpha_{\text{cure}}}} \tag{10}$$

where $\Gamma(x)$ denotes the gamma function [29, Ch. 6], $\alpha_{\text{inf}}$ is the infection time shape parameter, $\alpha_{\text{cure}}$ is the curing time shape parameter, and $b_{\text{cure}}$ is the curing time scale parameter (see Supplementary Note 1 for the derivation).

In Supplementary Note 2, we assess the validity of (10) on different graphs (Supplementary Table S1) through computer simulations. On the complete graph, the measured generation times in simulations closely follows (10). On sparser graphs, (10) becomes less accurate because the assumption of a constant number of susceptible neighbors becomes worse due to the smaller number of neighbors (Supplementary Fig. S1). However, simulations show that on sparse graphs, (10) is accurate in the shape but not the scale, meaning that the error between (10) and the measurements can be almost completely removed by tuning the scale parameter $b_{\text{cure}}$ (Supplementary Figs. S2–S4). Hence, (10) accurately describes the shape of the probability density of measured generation times, regardless of graph topology. Figure 2 shows a comparison of (10) with the measured density function of the generation time from computer simulations of a Weibull SIS process on the complete graph of $N = 100$ nodes for several infection time shape parameters. The solid lines show the theoretical density function (10) of the generation time and the points show the measured density from the simulation, which closely follows the theory.

In studies of biological epidemics, measured generation times are often fitted to a Weibull probability density function $\widehat{f}_{T_{\text{gen}}}(x)$ with shape parameter $\alpha_{\text{gen}}$. We therefore need to understand how the fitted generation time shape parameter $\alpha_{\text{gen}}$ is related to the underlying infection time shape parameter $\alpha_{\text{inf}}$ and curing time shape parameter $\alpha_{\text{cure}}$. We consider infection time and curing time shape parameters in the range $\alpha_{\text{inf}}, \alpha_{\text{cure}} \in \{0.3, 0.4, \ldots, 3.0\}$ and set the curing time scale parameter arbitrarily as

$$b_{\text{cure}} = \frac{\Gamma\left(\frac{\alpha_{\text{inf}}}{\alpha_{\text{cure}}}\right)}{\Gamma\left(\frac{\alpha_{\text{inf}}+1}{\alpha_{\text{cure}}}\right)}$$

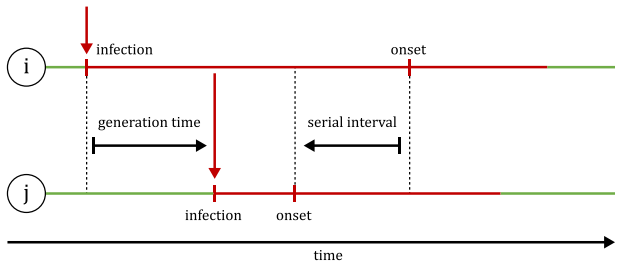



**Fig. 1 | Timeline illustrating the generation time and serial interval.** Node $i$ and node $j$ are both initially susceptible, indicated by green on the timeline. Node $i$ then becomes infected, indicated by red on the timeline. The red arrow indicates the infection event. Node $i$ then infects node $j$. The time difference between the infection events is the generation time, which is always positive. If people can transmit the disease before symptom onset, then the symptom onset of node $i$ may possibly occur after that of node $j$, as illustrated in this example. The serial interval, defined as the time difference between symptom onset, may then be negative.

such that the mean generation time $\mathbb{E}\left[T_{\text{gen}}\right] = 1$. We then fit a Weibull probability density function $\widehat{f}_{T_{\text{gen}}}(x)$ to (10). Figure 3a shows the fitted generation time shape parameter $\alpha_{\text{gen}}$ and Fig. 3b shows the error $\epsilon$ defined as the total variation distance (TVD) between the probability densities

$$\epsilon = \frac{1}{2}\int_0^\infty \left| f_{T_{\text{gen}}}(x) - \widehat{f}_{T_{\text{gen}}}(x) \right| \mathrm{d}x$$

If the infection time shape parameter and curing time shape parameter are the same, $\alpha_{\text{inf}} = \alpha_{\text{cure}}$, then (10) is precisely a Weibull distribution. Therefore, on the diagonal of Fig. 3a, the generation time shape parameter $\alpha_{\text{gen}} = \alpha_{\text{inf}} = \alpha_{\text{cure}}$ and the total variation distance is 0 on the diagonal of Fig. 3b.

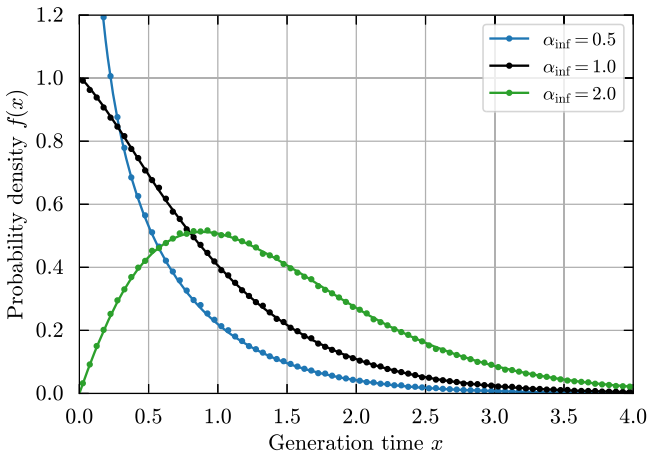



**Fig. 2 | Comparison of the theoretical density function of the generation time with the measured density from computer simulations.** The theoretical density function $f_{T_{\text{gen}}}(x)$ is indicated by the solid lines and the measured density is indicated by the points. Both the infection time $T_{\text{inf}}$ and curing time $T_{\text{cure}}$ are Weibull distributed. Three infection time shape parameters $\alpha_{\text{inf}} \in \{0.5, 1, 2\}$ are considered, while the curing time shape parameter is kept at $\alpha_{\text{cure}} = 1.3$. The scale parameters $b_{\text{inf}}$ and $b_{\text{cure}}$ are set such that the mean infection time $\mathbb{E}\left[T_{\text{inf}}\right] = 0.5$ and the mean curing time $\mathbb{E}\left[T_{\text{cure}}\right] = 1$ respectively. The simulations are performed on a complete graph of $N = 100$ nodes. The SIS process is modified to remove the all-healthy absorbing state by preventing the last infectious node from curing as in[32]. Each measured histogram is built from $10^6$ measurements of the generation time.

If the infection time shape parameter and curing time shape parameter are different, then (10) can be approximately described by a Weibull distribution with the generation time shape parameter $\alpha_{\text{gen}}$ somewhere between the infection time shape parameter $\alpha_{\text{inf}}$ and curing time shape parameter $\alpha_{\text{cure}}$. When moving away from the diagonal of Fig. 3, the difference between the infection time shape parameter $\alpha_{\text{inf}}$ and curing time shape parameter $\alpha_{\text{cure}}$ increases and so does the error. In Supplementary Figs. S5–S6, we fit measured generation times from computer simulations with a Weibull distribution. The results are consistent with Fig. 3 and the fitted generation time shape parameter $\alpha_{\text{gen}}$ is not affected by graph topology.

The generation time shape parameter $\alpha_{\text{gen}}$ increases when the infection time shape parameter $\alpha_{\text{inf}}$ or curing time shape parameter $\alpha_{\text{cure}}$ increases. The green cells in Fig. 3a show when the fitted generation time shape parameter $\alpha_{\text{gen}} > 1$, which almost always occurs when the infection time shape parameter $\alpha_{\text{inf}} > 1$. This is intuitive because a Weibull distribution with $\alpha_{\text{gen}} > 1$ is bell-shaped and (10) is bell-shaped when $\alpha_{\text{inf}} > 1$. Hence, if the generation time $T_{\text{gen}}$ can be approximately described by a Weibull distribution with shape parameter $\alpha_{\text{gen}} > 1$, then the underlying Weibull SIS process likely has infection time shape parameter $\alpha_{\text{inf}} > 1$.

If the infection time shape parameter $\alpha_{\text{inf}}$ is less than 1, then it is possible that the fitted generation time shape parameter $\alpha_{\text{gen}} > 1$ if the curing time shape parameter $\alpha_{\text{cure}}$ is sufficiently large. Realistically, a Weibull SIS process with an infection time $\alpha_{\text{inf}} < 1$ cannot yield a generation time shape parameter $\alpha_{\text{gen}}$ substantially larger than 1 because if $\alpha_{\text{cure}} \gg \alpha_{\text{inf}}$, then the generation time density (10) cannot be modeled with a Weibull distribution. This can be seen in Fig. 3a where the black outline shows when the TVD $\epsilon < 0.05$. If we consider the entries where the infection time shape parameter $\alpha_{\text{inf}} \leq 1$ and TVD $\epsilon < 0.05$, then the largest fitted generation time shape parameter $\alpha_{\text{gen}} = 1.3$. Therefore, if the generation time shape parameter $\alpha_{\text{gen}}$ is substantially larger than 1, then we can be almost certain that the underlying Weibull SIS process has infection time shape parameter $\alpha_{\text{inf}} > 1$.

## Measurements of the generation time shape parameter $\alpha_{\text{gen}}$ for several diseases

The Weibull distribution (4) is a commonly accepted distribution to approximate generation times measured in biological epidemics. Our idea is to measure the generation time shape parameter $\alpha_{\text{gen}}$ as a characterizer of non-Markovianity in biological epidemics. In Supplementary Table S2, we

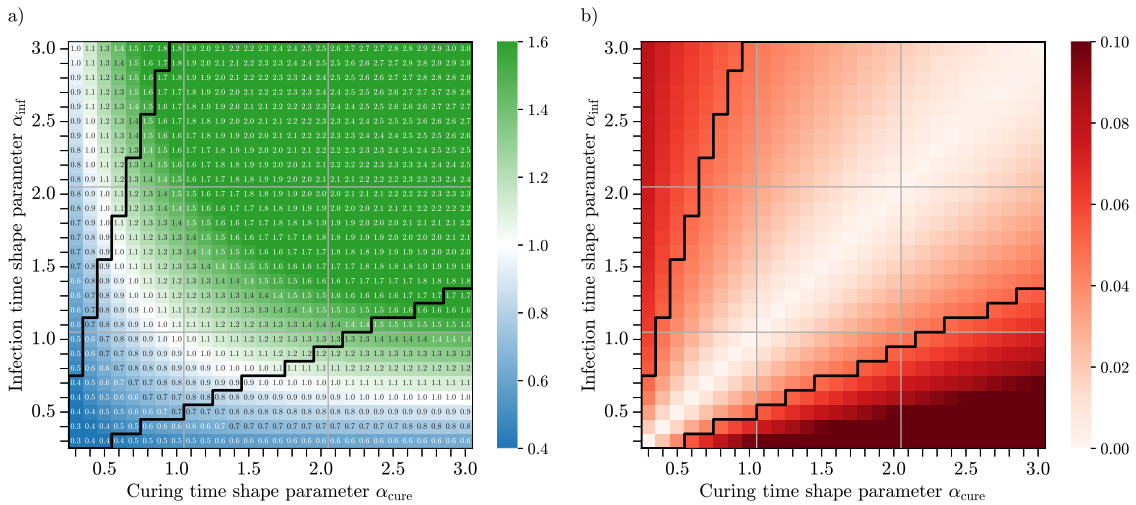



**Fig. 3 | Shape parameter and error when fitting the theoretical density function of the generation time with a Weibull distribution. a** Fitted generation time shape parameter $\alpha_{\text{gen}}$. White indicates $\alpha_{\text{gen}} = 1$, green indicates $\alpha_{\text{gen}} > 1$, and blue indicates $\alpha_{\text{gen}} < 1$. **b** Corresponding error of the Weibull fit, defined as the total variation distance $\epsilon = \frac{1}{2}\int_0^\infty \left| f_{T_{\text{gen}}}(x) - \widehat{f}_{T_{\text{gen}}}(x) \right| \mathrm{d}x$ between the theoretical density function $f_{T_{\text{gen}}}(x)$ and the fitted Weibull density function $\widehat{f}_{T_{\text{gen}}}(x)$. Darker shades of red indicate higher error. The black outline in each panel shows where the total variation distance $\epsilon < 0.05$.

have extracted the shape parameter $\alpha_{gen}$ from a large number of published biological disease measurements (in total 126). Details on the data collection and method for extracting the shape parameter are presented in Supplementary Notes 3–4 and Supplementary Figs. 7–8. If the publication reports the raw data, then we fit a Weibull distribution to the reported data. Otherwise, we infer the Weibull shape parameter from the reported mean and standard deviation.

A histogram of the shape parameters is plotted in Fig. 4. Generation times or serial intervals measured in biological respiratory epidemics typically exhibit a bell shape, corresponding to a shape parameter of $\alpha_{gen} > 1$ when fitted with a Weibull distribution.

Available empirical data suggests that $\alpha_{gen} < 1$ is not biologically plausible for generation times of person-to-person infectious diseases. In a human challenge study of influenza, investigators experimentally infect people with live influenza virus. In a review of human challenge studies, Carrat et al.[30] showed that the day after infection, people begin shedding influenza virus from their respiratory tract, and they showed that the amount of shedding peaks two days after infection. These findings are consistent with a relatively low probability density of short generation intervals, such as the Weibull distribution with a shape parameter $\alpha_{gen} > 1$. In a case-ascertained household study, people seek care for an illness; and later, investigators visit the home to collect information from all members of the household. In a careful analysis of serial intervals of influenza virus infection from a case-ascertained household study, Cowling et al.[19] found the best fit was a Weibull distribution with a mean of 3.6 days and a standard deviation of 1.6 days. This translates to a shape parameter of about $\alpha_{gen} = 2.4$. Chowell and Nishiura[20] fit a Weibull distribution to serial intervals for Ebola virus disease. They found a mean serial interval of 12 days with a shape parameter of $\alpha_{gen} = 2.6$, with a 95% confidence interval of 1.8–3.5. Vink, Bootsma and Wallinga[31] present a systematic review of all serial interval data published as of 1 October, 2013 about influenza, respiratory syncytial virus, severe acute respiratory syndrome, measles, varicella, smallpox, mumps, rubella, pertussis, and tuberculosis. By matching the mean and variance of their results to a Weibull distribution, we again find that the shape parameter $\alpha_{gen} > 1$.

In the previous section, we demonstrated that a Weibull distributed generation time $T_{gen}$ with shape parameter $\alpha_{gen}$ implies a comparable shape parameter $\alpha_{inf}$ for a Weibull distributed infection time $T_{inf}$. In other words, if $\alpha_{gen} > 1$, then it holds that $\alpha_{inf} > 1$, and vice versa, if $\alpha_{gen} < 1$, then it holds that $\alpha_{inf} < 1$. Hence, in biological and mainly respiratory epidemics, measurements in Fig. 4 reveal that the infection time $T_{inf}$ typically has shape parameter $\alpha_{inf} > 1$, corresponding to a slower spread than Markovian epidemics ($\alpha_{inf} = 1$).

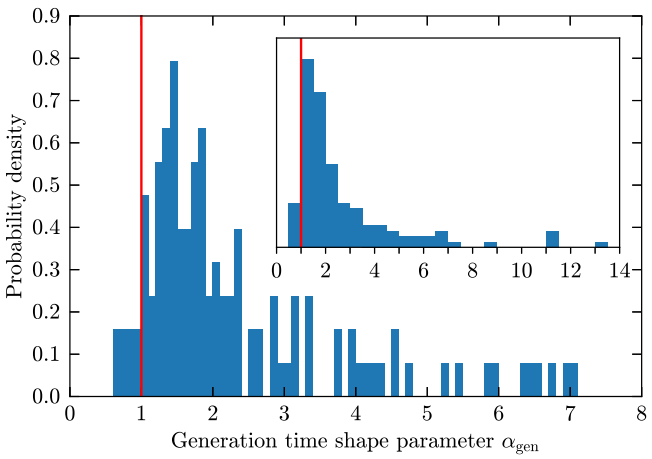



**Fig. 4 | Histogram of generation time shape parameters collected from the epidemiological literature.** The main figure uses a bin width of 0.1 and shows values up to $\alpha_{gen} = 8$. The inset uses a bin width of 0.5 and shows the full range of results. The red line in the main figure and inset indicates $\alpha_{gen} = 1$. Generation time shape parameter $\alpha_{gen} > 1$ implies an infection time shape parameter $\alpha_{inf} > 1$ in the underlying SIS process and thus a slower disease spread compared to the Markovian case ($\alpha = 1$).

## Conclusions

After explaining Markovian and non-Markovian SIS epidemic theory, we conclude that a generation time shape parameter $\alpha_{gen} > 1$ implies an infection time shape parameter $\alpha_{inf} > 1$ when modeled with a Weibull distribution. The non-Markovian SIS infection probability with $\alpha > 1$ is upper bounded by the Markovian ($\alpha = 1$) nodal infection probability and the basic reproduction number with $\alpha > 1$ is upper bounded by the Markovian ($\alpha = 1$) basic reproduction number (while the corresponding epidemic threshold is lower bounded by the Markovian mean-field epidemic threshold $\tau_c^{(1)} = \frac{1}{\lambda_1}$). A literature survey of published generation times and serial intervals in real-world person-to-person infections reveals that the shape parameter $\alpha > 1$ in most cases. Hence, Markovian models provide a safe upper bound.

The literature survey includes primarily respiratory pathogens, no sexually transmitted infections, and no blood-borne infections. Therefore, the development of a still missing $0 < \alpha < 1$ non-Markovian theory for biological respiratory epidemics does not seem needed anymore. For some infections, such as HIV, the idea of a bell-shaped distribution ($\alpha > 1$) for generation time might be more contentious. Hence, our claim only holds for pathogens spread by respiratory droplets, but not for all biological diseases. A practical limitation is that our theory is based on the generation time shape parameter $\alpha_{gen}$ while in practice, serial intervals are often measured. In cases where serial intervals are a poor proxy for generation times, one should not assume that the shape of the serial interval is comparable to that of the generation time; the distribution of the generation time should be recovered before drawing any conclusions about the underlying infection process. Finally, we have confined our treatment to SIS epidemics which upper-bound SIR epidemics in the nodal infection probability and in the basic reproduction number. For diseases where re-infections are rare, the SIS bounds may be excessively safe and therefore not of practical use when deciding on intervention measures in real-world epidemics.

## Data availability

The data that support the findings of this study are available from the corresponding author upon request.

Received: 1 October 2025; Accepted: 5 June 2026;
Published online: 23 June 2026

## References

1. Kermack, W. O. & McKendrick, A. G. A contribution to the mathematical theory of epidemics. *Proc. R. Soc. Lond. A* **115**, 700–721 (1927).
2. Darabi Sahneh, F., Scoglio, C. & Van Mieghem, P. Generalized epidemic mean-field model for spreading processes over multilayer complex networks. *IEEE/ACM Trans. Netw.* **21**, 1609–1620 (2013).
3. Van Mieghem, P., Darabi Sahneh, F. & Scoglio, C. An upper bound for the epidemic threshold in exact Markovian SIR and SIS epidemics on networks. In *53rd IEEE Conference on Decision and Control*, 6228–6233 (Los Angeles, CA, USA, 2014).
4. Van Mieghem, P. Exact Markovian SIR and SIS epidemics on networks and an upper bound for the epidemic threshold. *arXiv:1402.1731*. https://arxiv.org/abs/1402.1731. (2014).
5. Prasse, B. & Van Mieghem, P. Predicting network dynamics without requiring the knowledge of the interaction graph. *Proc. Natl. Acad. Sci.* **119**, e2205517119 (2022).
6. D'Alessandro, M. & Van Mieghem, P. Fractional derivative in continuous-time Markov processes and applications to epidemics in networks. *Phys. Rev. Res.* **7**, 013017 (2025).
7. Almasan, A.-D., Shvydun, S., Scholtes, I. & Van Mieghem, P. Generating temporal contact graphs using random walkers. *IEEE Trans. Netw. Sci. Eng.* **12**, 1649–1659 (2025).

8. Shvydun, S., Almasan, A.-D. & Van Mieghem, P. Temporal graph reproduction with RWIG. *IEEE Trans. Netw. Sci. Eng.* **12**, 3015–3024 (2025).
9. Van Mieghem, P. *Performance Analysis of Complex Networks and Systems* (Cambridge University Press, 2014), second edn.
10. Cator, E. & Van Mieghem, P. Second-order mean-field susceptible-infected-susceptible epidemic threshold. *Phys. Rev. E* **85**, 056111 (2012).
11. Van Mieghem, P., Omic, J. & Kooij, R. Virus spread in networks. *IEEE/ACM Trans. Netw.* **17**, 1–14 (2009).
12. Van Mieghem, P. The N-intertwined SIS epidemic network model. *Computing* **93**, 147–169 (2011).
13. Van Mieghem, P. & van de Bovenkamp, R. Accuracy criterion for the mean-field approximation in susceptible-infected-susceptible epidemics on networks. *Phys. Rev. E* **91**, 032812 (2015).
14. Van Mieghem, P. *Graph Spectra for Complex Networks* (Cambridge University Press, 2023), second edn.
15. Van Mieghem, P. & van de Bovenkamp, R. Non-Markovian infection spread dramatically alters the susceptible-infected-susceptible epidemic threshold in networks. *Phys. Rev. Lett.* **110**, 108701 (2013).
16. Prasse, B., Devriendt, K. & Van Mieghem, P. Clustering for epidemics on networks: A geometric approach. *Chaos: Interdiscip. J. Nonlinear Sci.* **31**, 063115 (2021).
17. Prasse, B. & Van Mieghem, P. Time-dependent solution of the NIMFA equations around the epidemic threshold. *J. Math. Biol.* **81**, 1299–1355 (2020).
18. Rinne, H. *The Weibull Distribution: A Handbook* (Chapman and Hall/CRC, New York, NY, 2008).
19. Cowling, B. J., Fang, V. J., Riley, S., Peiris, J. S. M. & Leung, G. M. Estimation of the serial interval of influenza. *Epidemiology* **20**, 334–347 (2009).
20. Chowell, G. & Nishiura, H. Transmission dynamics and control of Ebola virus disease (EVD): a review. *BMC Med.* **12**, 196 (2014).
21. Backer, J. A. et al. Shorter serial intervals in SARS-CoV-2 cases with Omicron BA.1 variant compared with Delta variant, the Netherlands, 13 to 26 December 2021. *Eurosurveillance* **27**, 220042 (2022).
22. Nishiura, H., Linton, N. M. & Akhmetzhanov, A. R. Serial interval of novel coronavirus (COVID-19) infections. *Int. J. Infect. Dis.* **93**, 284–286 (2020).
23. Van Mieghem, P. *The Mittag-Leffler and Gamma function* (Oxford University Press, 2026).
24. Boguñá, M., Lafuerza, L. F., Toral, R. & Serrano, M. A. Simulating non-Markovian stochastic processes. *Phys. Rev. E* **90**, 042108 (2014).
25. Svensson, A. A note on generation times in epidemic models. *Math. Biosci.* **208**, 300–311 (2007).
26. Park, S. W., Champredon, D. & Dushoff, J. Inferring generation-interval distributions from contact-tracing data. *J. R. Soc. Interface* **17**, 20190719 (2020).
27. Pellis, L., Ferguson, N. M. & Fraser, C. Epidemic growth rate and household reproduction number in communities of households, schools and workplaces. *J. Math. Biol.* **63**, 691–734 (2011).
28. Britton, T. & Scalia Tomba, G. Estimation in emerging epidemics: biases and remedies. *J. R. Soc., Interface* **16**, 20180670 (2019).
29. Abramowitz, M. & Stegun, I. A. *Handbook of Mathematical Functions* (Dover, New York, NY, 1968).
30. Carrat, F. et al. Time lines of infection and disease in human influenza: A review of volunteer challenge studies. *Am. J. Epidemiol.* **167**, 775–785 (2008).
31. Vink, M. A., Bootsma, M. C. J. & Wallinga, J. Serial intervals of respiratory infectious diseases: A systematic review and analysis. *Am. J. Epidemiol.* **180**, 865–875 (2014).
32. Cator, E. & Van Mieghem, P. Susceptible-infected-susceptible epidemics on the complete graph and the star graph: Exact analysis. *Phys. Rev. E* **87**, 012811 (2013).


## Acknowledgements

We thank F. Scott Dahlgren for his contributions to the literature overview of generation times. We thank Sang Woo Park, Bryan T. Grenfell, Simon A. Levin, H. Vincent Poor, Marián Boguñá and Jacco Wallinga for their feedback.

## Author contributions

B.L.C. and P.V.M. contributed equally to this work. P.V.M. conceived the study. B.L.C. and P.V.M. designed research. B.L.C. performed simulations. B.L.C. and P.V.M. wrote the paper.

## Funding

This research has been funded by the European Research Council (ERC) under the European Union's Horizon 2020 research and innovation programme (grant agreement No 101019718).

## Competing interests

The authors declare no competing interests.

## Additional information

**Supplementary information** The online version contains supplementary material available at https://doi.org/10.1038/s42005-026-02723-3.

**Correspondence** and requests for materials should be addressed to Brian L. Chang.

**Peer review information** *Communications Physics* thanks Giulio Burgio, Andrés Guzmán and the other, anonymous, reviewer for their contribution to the peer review of this work. A peer review file is available.

**Reprints and permissions information** is available at http://www.nature.com/reprints

**Publisher's note** Springer Nature remains neutral with regard to jurisdictional claims in published maps and institutional affiliations.

**Open Access** This article is licensed under a Creative Commons Attribution-NonCommercial-NoDerivatives 4.0 International License, which permits any non-commercial use, sharing, distribution and reproduction in any medium or format, as long as you give appropriate credit to the original author(s) and the source, provide a link to the Creative Commons licence, and indicate if you modified the licensed material. You do not have permission under this licence to share adapted material derived from this article or parts of it. The images or other third party material in this article are included in the article's Creative Commons licence, unless indicated otherwise in a credit line to the material. If material is not included in the article's Creative Commons licence and your intended use is not permitted by statutory regulation or exceeds the permitted use, you will need to obtain permission directly from the copyright holder. To view a copy of this licence, visit http://creativecommons.org/licenses/by-nc-nd/4.0/.

© The Author(s) 2026